

Radioactivity of MINOS detector components and environment; estimation of counting rates in the Far Detector

Keith Ruddick
University of Minnesota

The radioactivity of all components in the MINOS detector has been measured. The contributions from the ^{238}U and ^{232}Th decay chains have been identified, along with ^{40}K and ^{60}Co . These data have been combined with the previously measured radioactivity of the local Soudan rock to predict counting rates in the scintillator planes and also the rates of double and triple coincidences between different planes.

1. Introduction

Natural radioactivity provides a number of potential sources of background counts in any detector and these have been described in previous NuMI notes (L-210 and -313). This updates those notes, and includes rates predicted in the final MINOS geometry.

Table 1 shows the main sources of possible radioactivity in the earth's environment and, potentially, in the materials of the detector components. The table also shows the maximum energies involved in these decays. (A minimum ionizing particle going through a 1 cm strip of the MINOS scintillator deposits ~ 1.8 MeV on average) (The 2.39 and 3.94 γ s in the U and Th chains are actually the sum of branching fractions of a great many different γ s which occur in these decay chains).

Table 1. Principal sources of natural radioactivity in MINOS.

Isotope	Half-life (yr)	Decay mode	Max energy (MeV)	Comments
^{40}K	1.25×10^9	γ (10.5%)	1.461	.0117% of natural K
		β (89.5%)		(K is $\sim 1\%$ in earth)
^{232}Th	14.1×10^9	Decay chain to ^{208}Pb :		few ppm in earth
		6 α		
		4 β	2.25	
		2.39 γ	2.62	
^{238}U	4.46×10^9	Decay chain to ^{206}Pb :		few ppm in earth
		8 α		
		6 β	3.27	
		3.94 γ	2.20	
^{60}Co	5.27	2 γ	1.173, 1.332	Used in steel manuf.
		β	0.32	

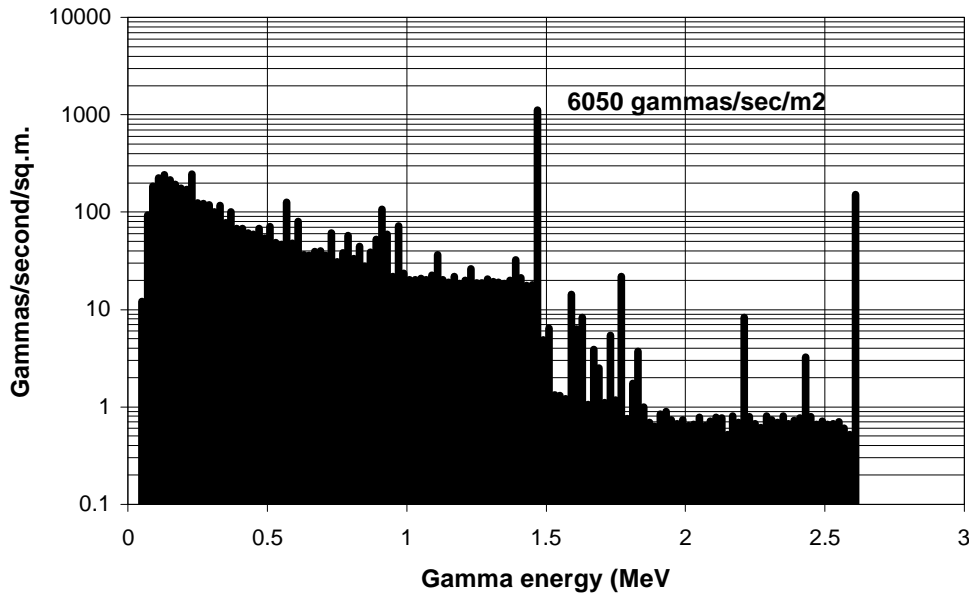
2. Review of rock radioactivity

γ -rays produced by U, Th and K decay in the rocks can produce knock-on electrons in the MINOS scintillators via Compton scattering, primarily. (Electrons emitted from the rock-walls are few and, anyway, have negligible probability of reaching the detector; in contrast, a 1 MeV γ -ray has an attenuation length of ~ 200 m in air).

As described in earlier NuMI notes, I carried out a survey of the Ely Greenstone and shotcrete activity in the early days of the Soudan-2 detector. Samples of rock were obtained from several different areas of the excavation and analyzed using a shielded sodium iodide crystal in our lab in Minneapolis. The detector/sample geometry was calibrated with a known mass of thorium metal, potassium salts, and a piece of pitchblende (uranium ore). Standard analysis techniques were used to extract the concentrations of U, Th and K in all the samples. The results have been described in NuMI L-210 and L-313. Counting rates predicted there have been updated in this note, using the actual MINOS geometry - the plane pitch is larger than originally assumed.

Using the measured isotopic concentrations, I have used a Monte Carlo program to generate the raw γ spectrum produced by the U and Th and K decays. These γ s are followed as they Compton scatter and are eventually completely absorbed via the photoelectric effect. Figure 1 shows the calculated spectrum of γ s leaving the rock face. The most prominent peaks are due to ^{40}K (1.461 MeV) and ^{208}Tl (2.615 MeV) from the thorium chain..

Figure 1. Gamma spectrum emerging from Soudan rock walls (inc. 2.5 cm shotcrete)

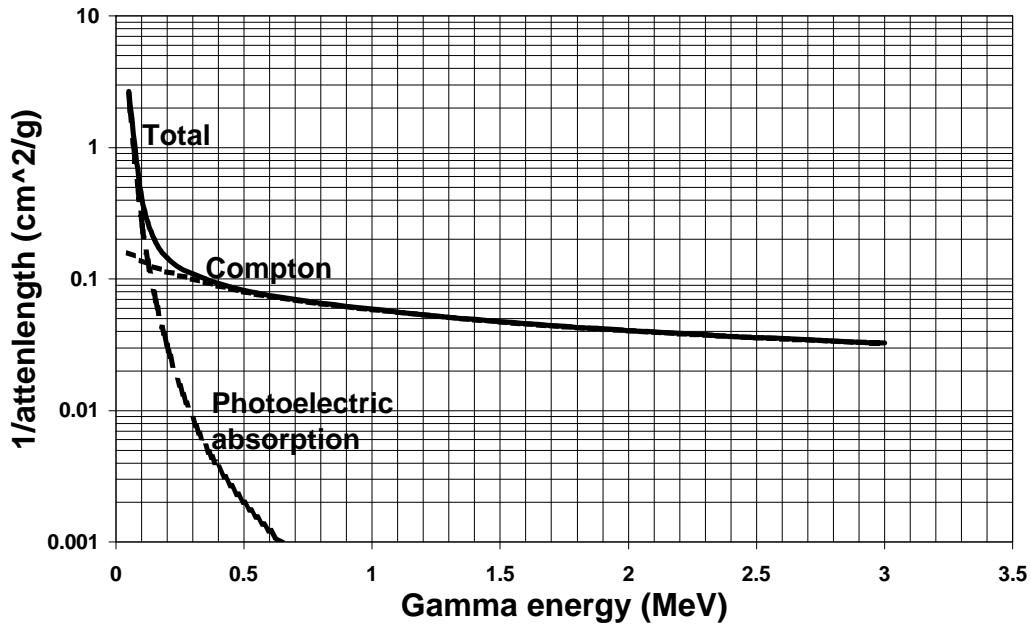


The counting rates predicted rates in the Soudan 2 shield agreed within 20% of the rates that were eventually measured.

3. Counting rate in the MINOS Far Detector

Figure 2 shows the attenuation length of γ s in iron for the processes of Compton scattering and photoelectric absorption separately. Over much of the energy range of interest, the attenuation length is about 20 g/cm^2 , i.e. one steel plate thickness. Photoelectric absorption in the scintillator is negligible (goes $\sim Z^4$) while the Compton attenuation length is essentially the same as in iron (goes like electron density). In the MINOS geometry, the presence of the steel absorber determines the lowest energies that are relevant: the steel becomes essentially opaque below about 100 keV due to the very rapid rise in the photoelectric cross-section. A good first estimate of the interaction rate in the active scintillator planes is given simply by the ratio of thicknesses, i.e. 1.0 g/cm^2 scintillator to 20 g/cm^2 iron $\approx 5\%$.

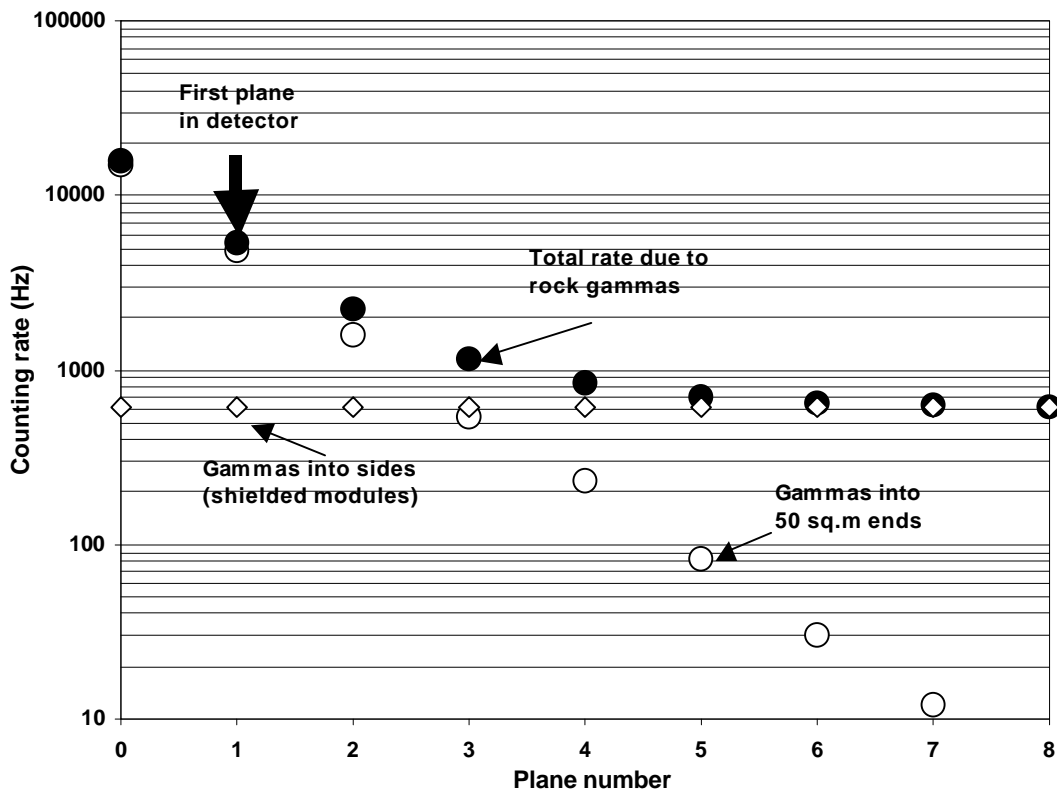
Figure 2. Gamma attenuation in iron



The Monte-Carlo is used to determine the energy deposited in the scintillator strips. In all calculations of the corresponding counting rates in the detector planes, I assume that the light output from the center of an 8 m long scintillator strip is 5 pe/mip from a single end, and that attenuation of this light along the wavelength shifting fiber is given by a sum of two exponentials: $(\exp(-x/\lambda_1) + \exp(-x/\lambda_2))$ with $\lambda_1 = 1$ m and $\lambda_2 = 8$ m. In addition, I add an extra 0.75 m to the fiber lengths to allow for the average fiber “tail” in the manifolds before the optical connector. I assume that there is no attenuation in the clear fibers beyond this point.

Figure 3 shows the predicted singles rate for the first few planes of the Far Detector due to this source of gammas. Note that “Plane-0” is for a plane unshielded on one side and that “Plane-1” is the actual first plane in the detector. This is the rate expected for single-ended readout – the rate for double ended, i.e. the OR of both sides of the Detector is essentially double these rates.

Figure 3. Singles rates in end planes of Far Detector (rock gammas)



I predicted that the first plane of the detector would have a singles rate of 5.6 kHz due to the rock radioactivity, and that after 5 or 6 planes (well into the detector, so that γ s only enter through the sides of the detector) the rate should be about 600 Hz for single-ended readout. When the first planes of the far detector were actually installed, the singles rates in the planes far exceeded these predicted rates! The rate was several kHz in the shielded planes. From the fact that the rate was fairly uniform across the planes, rather than severely attenuated away from the edges as predicted, it also appeared that the source is internal to the detector. An immediate program was started to identify the source of these extra counts.

In fact, nearly all of the extra counts appear as single photoelectrons in the MINOS photomultipliers. This is not at all characteristic of the products of the γ -rays from the likely sources: the identification and nature of this (non-radioactive) source was first recognized by Leon Mualem and will be described in a separate NuMI note. These single pe rates appear to be due to de-excitation of luminescence centers in the green WLS fibers, excited by mechanical handling of the active detector modules, and decaying with lifetimes of one or two months.

In addition to Leon's investigation of the fiber luminescence, γ -spectra of all components in the detector have been measured at Argonne National Laboratory and

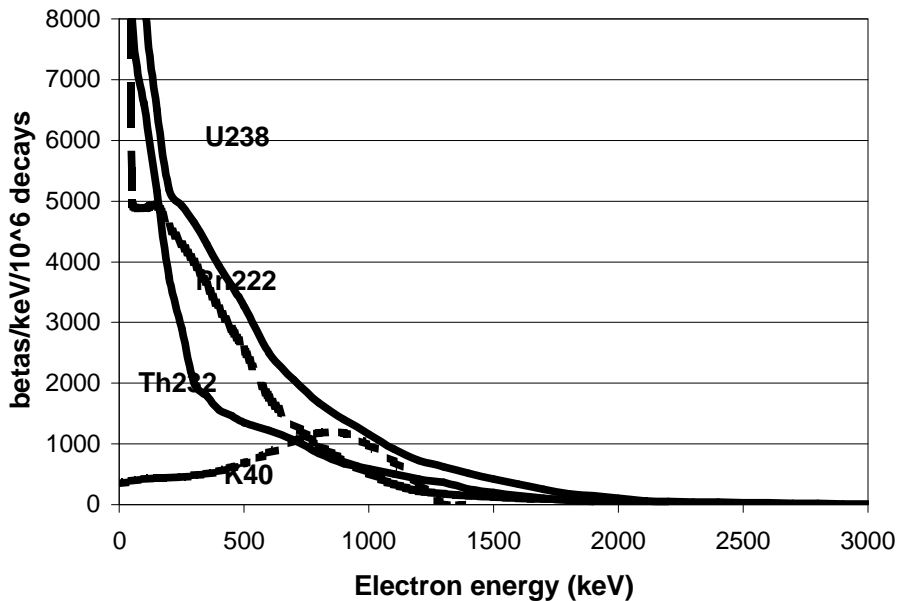
analyzed by me. (I was already analyzing the Argonne spectral data from samples of the steel used in the MINOS detectors – primarily to set limits on ^{60}Co contamination, which can lead to significant counting rates). As a result of these studies, several additional components of radioactivity in the detector materials have been found to give contributions comparable to that of the rock. Finally, significant amounts of radon (up to 30 picoCurie/liter) have been measured in the MINOS cavern and this contribution will also be calculated.

4. The effect of radon

^{222}Rn is produced through the α -decay of ^{226}Ra in the ^{238}U decay chain. It has a half-life of 3.8 days, its concentration depends on the local air circulation rate and also on atmospheric pressure. (There is another isotope of radon in the Th chain, but its half-life is only 55 s, so it doesn't have time to diffuse significantly out of the rock/shotcrete).

The radon decays through two successive α -decays in which the charged daughters, ^{218}Po ($\tau_{1/2} = 3\text{min}$) and ^{214}Pb ($\tau_{1/2} = 27\text{min}$), attach themselves to a local surface. This followed by two successive β -decays: ^{214}Pb to ^{214}Bi ($\tau_{1/2} = 20\text{min}$) to ^{214}Po . The relevant β -spectra are shown in Figure 4. These are actually the sums of all spectra emitted in the decay chains. (These spectral data can be obtained from <http://nucldata.nuclear.lu.se/nucldata> for example).

Figure 4. Beta spectra



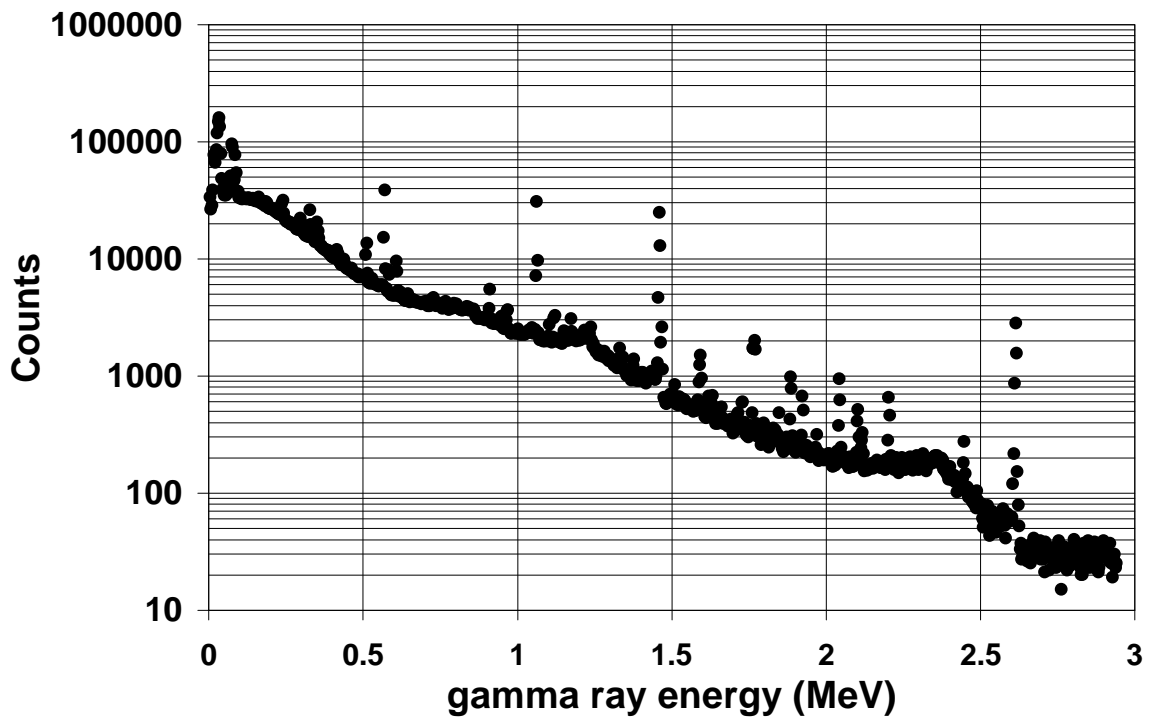
Accompanying the emitted β s are some γ s. The counting rates due to radon γ -rays were calculated using the same Monte-Carlo as used for the rock γ s. The rates are relatively enhanced because they occur between the detector planes. In addition the β

emitted directly in the decays also have a high probability to hit the scintillator planes directly; this is a significant component, although most are absorbed in the detector module covers, the epoxy layer, and the reflective layer on the scintillator. They have a significant effect on the rate of plane-to-plane coincidences, especially.

5. Measurements of the radioactivity of the MINOS detector components

A sample of every component used in the manufacture of the MINOS modules was obtained by Don Jankowski at Argonne and sent to their counting facility. That facility has several large intrinsic germanium detectors operating in a shielded environment. These detectors have energy resolution of a couple of keV and so are well able to resolve the many gammas emitted in the Th and U decay chains where the maximum energy is 2.615 MeV. A typical spectrum is shown in Figure 5.

Figure 5. A typical Ge detector spectrum



The ~400g samples were placed in standardized holders in standardized positions and absolute calibration of the detectors was done with a “cocktail” of standard gamma sources with known activity in the same geometry. There is an uncertainty of about 10% in the detector response with energy, due to counting statistics and different self-

absorption of gammas in the samples. Printouts of the raw spectra and calibration data were sent to me, along with background runs for each of the detectors used. These data runs were usually carried out for 240,000 seconds, i.e. over a whole weekend.

The procedure is to convert channel number (8192 total) to energy and then to identify the principal gammas to be expected, determine the number of gammas in the corresponding peaks for both sample and background, then to do a subtraction of these. (Note: for the uninitiated, these measurements are not simple. There are two backgrounds in the problem: one the background with no sample in place and also the “background” under a full-energy peak in a given spectrum. This latter is due to Compton scattered electrons from higher energy gammas. The background runs with no sample present show the same peaks as the samples, although at lower levels usually, since these ubiquitous Th, U and K gammas are also present in the environmental background and so have a finite chance of getting through the shielding. The samples themselves also provide some shielding: in the case of the steel measurements, for example, the sample rates are actually a few % lower than the background for this reason, and there is significant ^{60}Co in the background – none seen in the steel, yet, after subtraction).

Five or six γ -peaks in each of the Th and U chains were used to obtain a best estimate of the Th and U concentration in each of the samples. In all cases except one the decay chains were in equilibrium; the TiO₂ sample was out of equilibrium, i.e., rates from early in the chain disagreed with those later, presumably due to chemical processing of some sort.

The results of all analyses are shown in Table 2. The last column shows decay rates normalized to the mass of the sample per plane. The calculation of the corresponding singles rates per plane will be described later in this report.

6. Comments on the results of the measurements

The 2216 epoxy is used to attach the scintillator strips to the aluminum covers; it shows negligible activity and the upper limits are shown. Elsewhere in the table, the word “negligible” implies that the same result was obtained.

The DP190 epoxy was used on about 100 of the initial CalTech modules. It contains significant radioactivity due to the presence of a clay which is added to make it very viscous. We had already changed from this epoxy before these new measurements were made because it was several times more expensive and also because it required expensive mixers; the 2216 is quite viscous and is mixed by hand.

Table 2. Results of γ -ray analysis of MINOS components. The fourth column shows the actual results from the analysis and the fifth column the decay rates normalized to the number of decays per plane of Far Detector scintillator modules. These final numbers provide the basis for calculation of counting rates in the scintillators.

Material	Mass/plane	Isotope	Decay/kg/s	Decay/plane/s
TiO2	4.6 kg	²³² Th	0.69 ± .19	3.2 ± 0.9
		²³⁸ U	1.35 ± .30	6.2 ± 1.4
		⁴⁰ K	3.8 ± 2.3	17 ± 11
		⁶⁰ Co	0.62 ± .08	2.9 ± 0.4
2216 epoxy A	6.3 kg	²³² Th	< .09 (1σ)	< 0.6 (1σ)
		²³⁸ U	< .14	< 0.9
		⁴⁰ K	< 1.4	< 8.8
2216 epoxy B	6.3 kg	²³² Th	< .16	< 1.0
		²³⁸ U	< .28	< 1.8
		⁴⁰ K	< 2.1	< 13
DP190 epoxy A	7.5 kg	²³² Th	22.0 ± 2.0	165 ± 17
		²³⁸ U	10.2 ± 1.0	77 ± 8
		⁴⁰ K	18.4 ± 1.8	138 ± 14
DP190 epoxy B	7.5 kg	²³² Th	18.4 ± 1.8	138 ± 14
		²³⁸ U	7.5 ± 0.8	56 ± 6
		⁴⁰ K	10.2 ± 1.9	77 ± 8
EPON315C (optical epoxy)	2.5 kg	²³² Th	0.09 ± .19	0.23 ± 0.48
		²³⁸ U	0.85 ± .20	2.1 ± 0.5
		⁴⁰ K	2.8 ± 1.6	7.0 ± 4.0
		⁶⁰ Co	0.38 ± .06	0.95 ± .15
EPON hardnr (Teta)	0.4 kg		negligible	negligible
Aluminum	140 kg	²³² Th	4.6 ± 0.5	644 ± 70
		²³⁸ U	1.8 ± .18	252 ± 25
		⁴⁰ K	4.5 ± 7.3	630 ± 1000
WLS fibers	1.4 kg		negligible	negligible
RTV	0.7 kg		negligible	negligible
DP810	0.23 kg		negligible	negligible
Welding plugs	3.9 kg	²³² Th	2.5 ± 0.25	9.6 ± 1.0
		²³⁸ U	12.4 ± 1.2	48 ± 4.8
		⁴⁰ K	0.0 ± 2.4	0.0 ± 9.4
Steel plate	10,400 kg	⁶⁰ Co	.0018±. 0024	19 ± 32

While the aluminum covers appear to be very radioactive, they actually have an activity typical of many inorganic materials, i.e. a few ppm Th and U. Their significance comes from their large total mass of 140 kg per plane. The ⁴⁰K concentration in the aluminum is consistent with zero.

Samples of all the steel used in MINOS are tested for the presence of ^{60}Co which can produce a very pernicious background since it decays to two relatively high energy γ 's (1.17 and 1.33 MeV). There are no other significant sources seen in the steel spectra. The numbers shown in Table 1 are averaged over about 20 samples, corresponding to 32 kg steel. Clearly the most significant source of activity from the steel planes comes from the 76 welding plugs that contain significant U, especially. This is still small compared to the aluminum covers.

7. Calculation of rates in the detector

The following graphs show the results of my calculations of the counting rates in the detector. These include the contributions from β s as well as γ s. The (variable) radon rate has been taken to be 20 pCi/l. The addition of this radon component plus the radioactivity of the internal MINOS components doubles the predicted counting rates, approximately, although the γ s coming from the rock completely dominate at the edges.

Figure 6. Counting rate/strip - single-ended readout

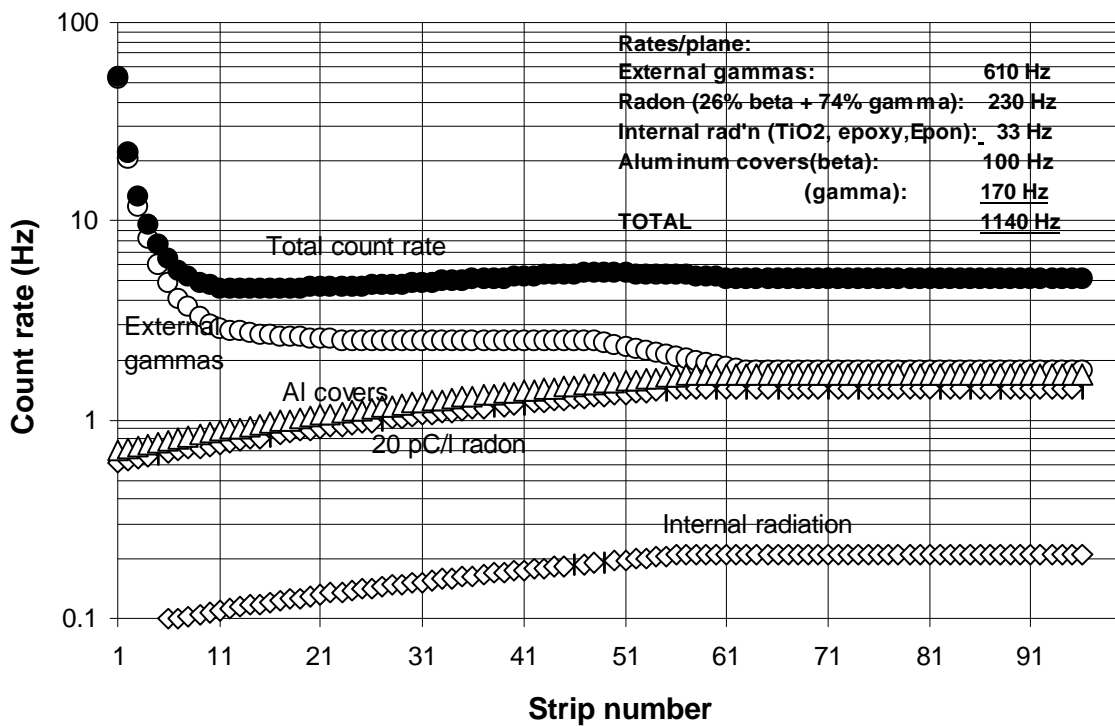


Figure 7. Counting rate per strip - opposite end coincidences

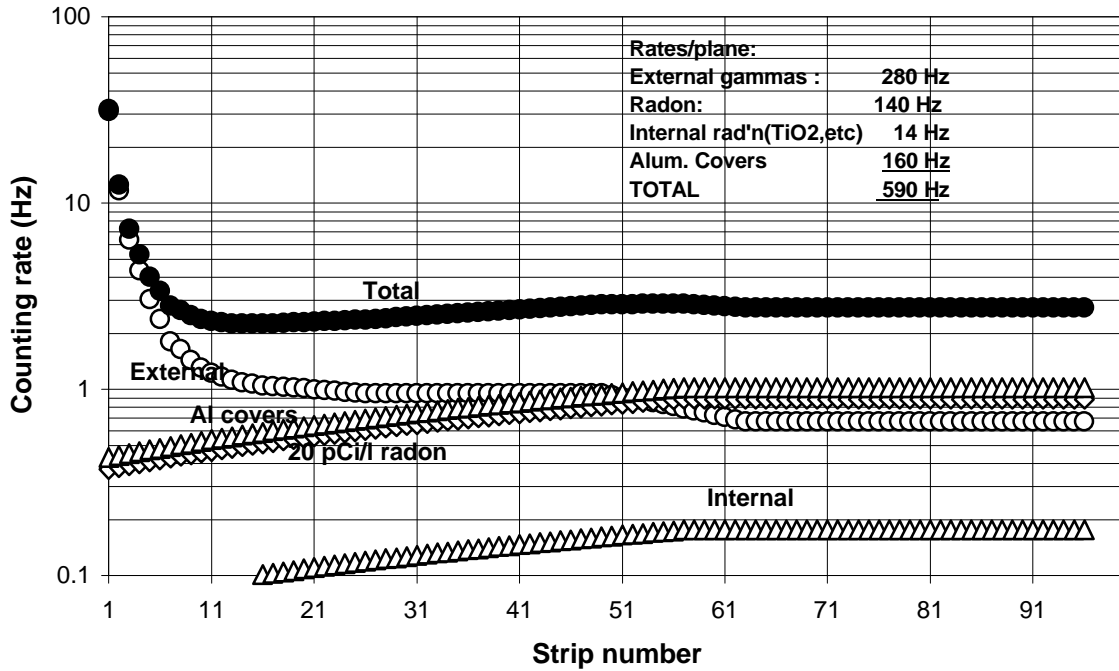
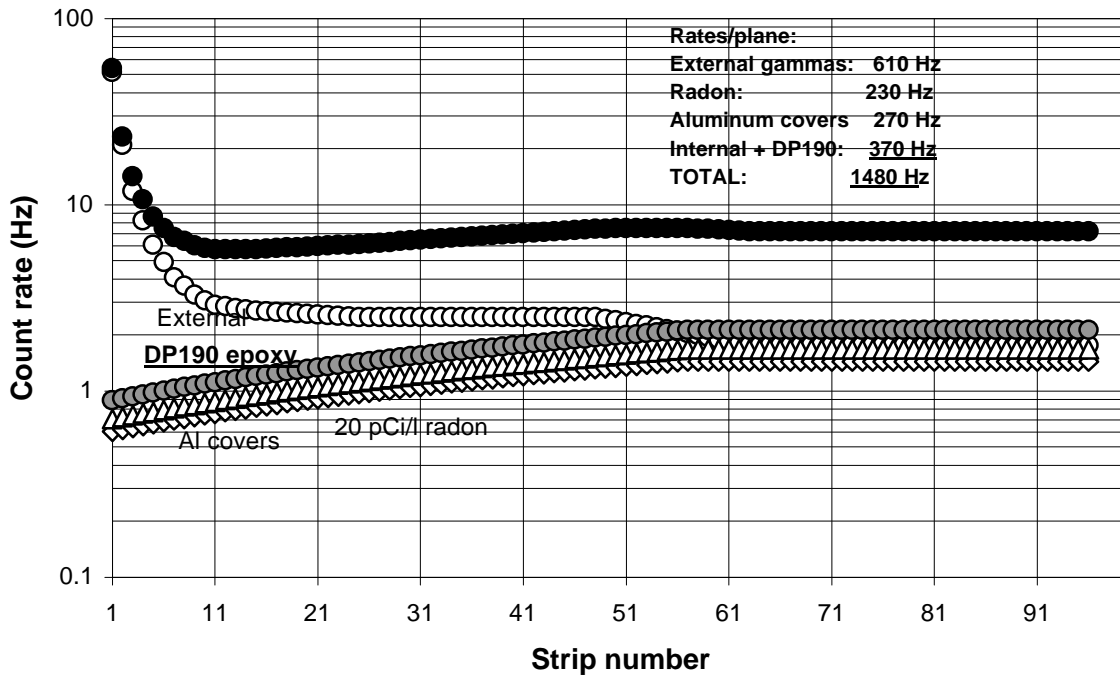


Fig 8. Counting rate/strip - single-ended - DP190 modules



8. Photoelectron spectra

Figure 9 shows the expected pulse-height distribution in a Hamamatsu M-16 phototube connected to an 8-m long scintillator strip. The contributions from the individual sources are also shown. These are: open circles – external γ s; open squares – γ s from Al covers; open triangles – ^{214}Bi γ s (radon); open diamonds - β s from Al covers; vertical crosses - ^{214}Bi β s (radon); angled crosses - ^{214}Pb γ s (radon); closed circles – total.

The average pulse height is 2.5 pe. This does not include any further attenuation in the clear fibers leading from the optical connectors on the detector modules to the phototubes.

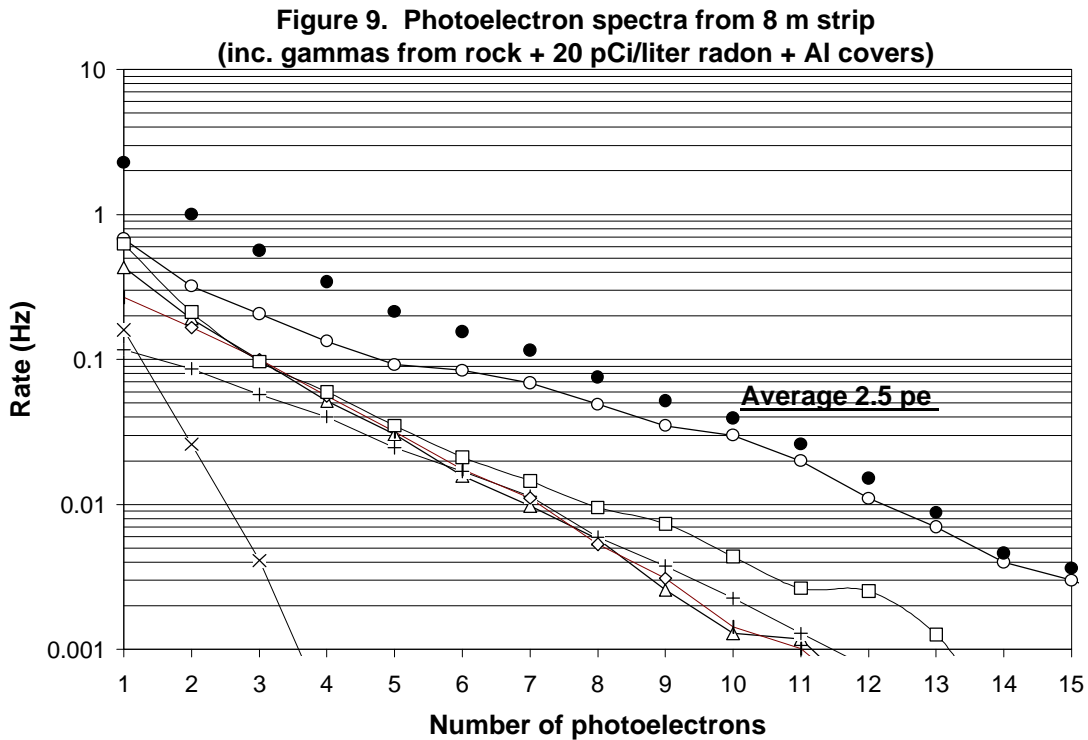
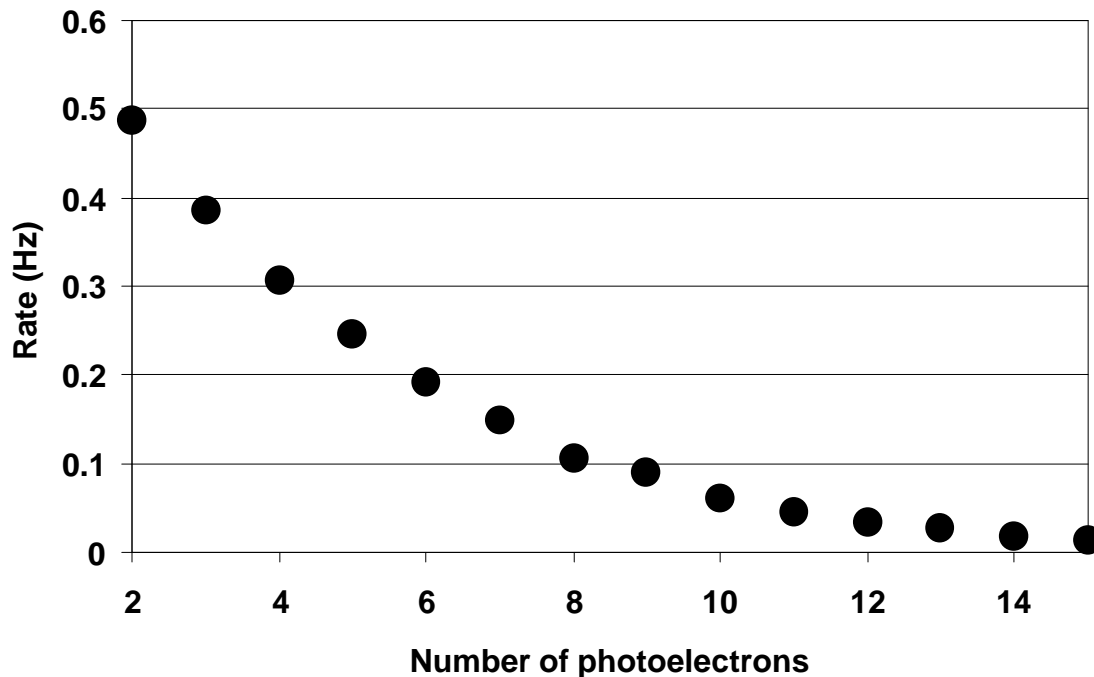


Figure 10 shows the summed pulse-heights for coincidences between opposite ends of the scintillator strips. For comparison, there are about 10 pe/minimum ionizing particle.

Figure 10. Photoelectron spectrum from 8 m strip
- summed, coincidences



9. Multi-plane coincidences

Finally, what is the probability for two or more planes to be hit simultaneously? There are two sources: multiple Compton scattering in different planes, originating from a single γ -ray; and a direct β hit from radon or an internal source plus one or more Compton scatters from its accompanying γ -ray. The tables below show the separate contributions.

Table 3. Double-coincidences between different planes. The numbers are predicted rates in Hz/plane.

Source	Single-sided	Side 1 OR Side 2	Side 1 AND Side 2
Rock γ	5.6	11.4	2.9
Internal γ	1.8	3.7	0.6
Internal β - γ	5.2	10.6	2.0
Radon γ (^{214}Bi)	1.0	2.0	0.2
Radon β - γ	1.8	3.6	0.6
Total	15	31	6.3

Table 4. Triple coincidences between different planes.

Source	Rate/plane (Hz)
Rock γ (3 Compton sc)	0.07
Internal γ (3 Compton)	0.02
Internal β - γ (β + 2Compton)	0.11
Radon β - γ (β + 2Compton)	0.017
Total	0.22

In these tables, “Rock γ ” refers to multiple Compton scatters from the radiation produced in the surrounding rock, “Internal γ ” refers to the same from sources in the detector materials, “ β - γ ” is coincidences between a direct β plus one or more Compton scatters in different scintillator planes. The rates for coincidences (AND) of sides and 2 are relatively low because these γ s typically make several scatters and have quite low energies as a consequence.

A significant approximation has been made in the calculation of the β - γ coincidences. There are actually many different β s emitted, each with their own energy spectrum and each with a characteristic γ -ray spectrum. To determine the true correlated β - γ coincidence rates would require each to be treated independently; instead, I have used averaged β -spectra to estimate the correlations. This probably is not too bad a method and is probably good to factor 2. To do it correctly is a very large project and not really worth the effort.

10. Conclusions

Based on experience with the Soudan 2 active shield and detector, the predicted counting rates should be correct within about 25%, although the double and triple coincidences will necessarily have larger errors. It should be remembered that the predicted rates are based on pulse-height distributions at the optical modules; there will be some small degradation of rate due to attenuation in the clear fibers that connect the optical modules to the phototubes.

One interesting question still existing is: How much signal persists from the green WLS fiber luminescence after a long time? Since this is a pure 1-photoelectron signal, it should be possible to estimate its persistence by inspection of the pulse-height spectra from single strips and by comparison with Figure 9. It should be straightforward to extract the non-radioactivity part of the signal.

Of course, requirement of a coincidence between opposite end of the strips removes the luminescence signal completely. Figure 7 represents this “clean” signal, due to radioactivity alone.

